JPP Journal of Pharmacy and Pharmacology

JPP 2005, 57: 973–980

Received February 11, 2005
Accepted April 25, 2005
DOI 10.1211/0022357056686
ISSN 0022-3573

Explaining the phase behaviour of the pharmaceutically relevant polymers poly(ethylene glycol) and poly(vinyl pyrrolidone) in semi-fluorinated liquids

Alison Paul, Peter C. Griffiths, Robert James, David J. Willock and Philippe G. Rogueda

Abstract

Phase behaviour studies of low molecular weight poly(ethylene glycol) (denoted PEG 600 and PEG 1000, corresponding to molecular weights of 600 and 1000 g mol^{-1}, respectively) have been carried out in 2H,3H-perfluoropentane (HPFP) with and without added poly(vinyl pyrrolidone). The concentration and temperature dependencies of their phase behaviour and the effect of moisture on these systems have been established. Furthermore, the solubility of PEG 600 in binary mixtures of HPFP and perfluoropentane (PFP), as well as HPFP and perfluorodecalin (PFD) have been considered at high HPFP contents. A phase separation phenomenon in fluorinated non-aqueous media is reported for the first time: PEG 600 and PEG 1000 both show a lower critical solution temperature type phase separation boundary. The size of the PEGs was obtained from small-angle neutron scattering (radius of gyration) and pulsed-gradient spin-echo NMR (hydrodynamic radius) measurements. It is shown that polymer conformation follows a regular trend with solution concentration; the size increases from <10 Å at 3 wt% in HPFP to 45 ± 2 Å at 20 wt% PEG. On changing the solvent composition by substitution of HPFP by PFP or PFD, the size decreases, consistent with a decrease in the hydrogen-bonding capacity of the solvent mixture. Computer modelling indicates an interaction between the PEG oxygen and the hydrogen of HPFP, an interaction that is absent for the fully fluorinated solvents. This indicates that hydrogen bonding is the driving force for polymer solubility in these solvents.

School of Chemistry, Cardiff University, Main Building, Park Place, Cardiff CF10 3AT, UK

Alison Paul, Peter C. Griffiths, Robert James, David J. Willock

AstraZeneca R&D Charnwood, Bakewell Road, Loughborough, Leicestershire LE11 5RH, UK

Philippe G. Rogueda

Correspondence: P. C. Griffiths, School of Chemistry, Cardiff University, Main Building, Park Place, Cardiff CF10 3AT, UK. E-mail: griffithspc@cardiff.ac.uk

Acknowledgements and funding: Financial support from AstraZeneca is gratefully acknowledged, as is access to the neutron facilities and the help provided by the respective instrument scientists (ISIS, S. M. King, R. K. Heenan; ILL, I. Grillo, R. Schweins).

Introduction

Fluorinated and partially fluorinated liquids have unique physical and chemical properties that distinguish them from their hydrocarbon equivalents. The larger size of fluorine compared to hydrogen causes greater stiffness of the fluorocarbon chains as they adopt a helical conformation, shielding the carbon chain from attack by reagents (Rigby & Bunn 1949). The enhanced strength of the C–C bond in fluorinated materials (e.g. 413 kJ mol^{-1} in perfluoroethane compared with 376.0 kJ mol^{-1} in ethane; Lide 1994) ensures a high level of chemical inertness, which makes them suitable for use in harsh chemical and physical environments and also makes them ideal candidates for use in biomedical applications, as reviewed by Krafft (2001) and Reiss (2002). Many fluorocarbons have been tested for biological activity and found to be non-toxic (Krafft et al 1998). There are many potential biomedical uses of fluorocarbon liquids, perfluorocarbons and systems that include them, for example as blood substitutes (Krafft & Reiss 1998; Reiss & Krafft 1999), for liquid ventilation (Wolfson et al 1996) and in drug delivery systems, including as propellants used in pressurized metered-dose inhalers (pMDIs) (Rogueda 2003). The very low polarizability of fluorine atoms means that perfluorocarbons exhibit only weak van der Waals interactions. This results in many of their unique properties, e.g. low surface tensions, low dielectric constants, high compressibilities, high gas solubilizing capabilities and low cohesive energy densities (Reed 1964; Reiss 1994; Krafft & Reiss 1998; Reiss & Krafft 1999). Furthermore hydrofluorocarbons (HFAs) are significantly less environmentally damaging than their fully halogenated chlorofluorocarbon (CFC) counterparts and accordingly are increasingly being used as

alternative solvents to CFCs. In the case of pMDIs (Rogueda 2003) this change in solvent necessitates a reformulation of the product.

The incompatibility of fluorocarbons with most types of material (they are strongly hydrophobic and also lipophobic) makes fluorinated liquids poor solvents. Most practical applications therefore rely on the use of a range of additives to turn them into viable product carriers. Although product performance can be measured and assessed, there is a lack of predictive and prescriptive tools to describe the behaviour of even commonly used excipients in these types of solvent. In order to achieve this, there is a need to understand the fundamental solution properties of polymers and surfactants in fluorinated and semi-fluorinated liquids. In this work we have chosen the partially fluorinated solvent 2H,3H-perfluoropentane (HPFP) – a suitable model for the HFA propellants used to replace CFCs in pMDI formulations (Rogueda 2003) combined with the simple polymers poly(ethylene glycol) (PEG) and poly(vinyl pyrrolidone) (PVP).

Materials and Methods

PEGs of average molecular weight 600 g mol^{-1} (PEG 600) or 1000 g mol^{-1} (PEG 1000), in conjunction with PVP of molecular weight 25 000–35 000 g mol^{-1} (PVP K25) and PVP of molecular weight 44 000–54 000 g mol^{-1} (PVP K30) were all purchased from Aldrich. PEG samples of differing molecular weights were also screened for HPFP solubility: 2000 g mol^{-1} and 4600 g mol^{-1}. Unless otherwise stated in the text, all polymers were oven dried to constant mass (typically 36 h at 70°C) and stored in a desiccator prior to use. HPFP (Apollo Scientific) was treated by shaking with acidic and then basic alumina followed by filtration. Where indicated the solvent was dried over molecular sieves. Deuterated PEG (molecular weight 800 g mol^{-1}) was obtained from the Manchester Polymer Group and used as received. Perfluoropentane (PFP) and perfluorodecalin (PFD) were obtained from Fluorochem and dried over molecular sieves. Before use HPFP, PFP and PFD were filtered through 0.8 μm cellulose filters (Minisart, Fisher). D_2O (99.9% d-atom) was used as received from Fluorochem. All other chemicals were from Aldrich and used as received.

Phase behaviour

Samples were prepared by mass on a 5-g scale in screw-capped glass vials sealed with Teflon tape. Where sample concentrations required an extremely small amount of polymer this was added to the vial first as a concentrated stock solution in ethanol and the other components were added after evaporation of the alcohol. Samples were mixed for 24 h at room temperature and then equilibrated at the experimental temperature in a circulating water bath (±0.1°C). To avoid hysteresis effects, phase boundaries were observed on cycling the temperature through heating, cooling and reheating. Generally it was sufficient to leave the samples for between 8 and 24 h at each temperature before visual inspection. For samples close to a phase boundary it was occasionally necessary to leave them for a longer time to equilibrate, up to 48 h. Samples were studied in duplicate. To establish the required equilibration time some PEG 1000 samples were left for up to 2 weeks, and their appearance did not change in the elapsed time between 48 h and 14 days. The temperature range studied was 15–40°C (the boiling point of HPFP is 54°C), at up to a maximum of 20 wt% polymer.

Determination of polymer solubilities

The solubility of the various PEGs was determined by a 'dry weights' assay. The (much lower) solubility of PVP was evaluated by spectophotometric analysis. A sample containing excess polymer was filtered to remove undissolved polymer and a known mass of the filtrate allowed to evaporate to dryness. A known mass of water was then added to dissolve the polymer and the concentration of this solution determined from the absorbance at 196 nm (Chaimberg & Cohen 1991). The calibration plot, measured at room temperature (20°C) in 10-mm quartz cells using water as the background, was found to obey Beer's law up to 40 ppm PVP.

Pulsed-gradient spin-echo nuclear magnetic resonance (PGSE-NMR)

PGSE-NMR experiments were performed as described previously (Griffiths et al 1997) on a Bruker AMX360 spectrometer, using a stimulated echo sequence in conjunction with current-regulated field gradient drivers and ramped gradient pulses. Three field gradient pre-pulses were applied before every scan to bring the effects of coil heating and eddy currents to a first-order steady state. Temperature stability was maintained to ±0.5°C.

For isotropic Brownian motion, the self-diffusion coefficient, D_s, is extracted by fitting the decay in signal given by the measured peak height, $A(\delta)$, as a function of field gradient pulse duration, δ, intensity, G, and separation, Δ, to equation 1:

$$A_{(G,\delta)} = A_{(0)} \exp -\left(\frac{\tau}{T_2}\right) \exp -(kD_s)^{\beta} \qquad (1)$$

where $k = -\gamma^2 G^2 \left(\frac{30\Delta(\delta+\sigma)^2 - (10\delta^3 + 30\sigma\delta^2 + 35\sigma^2\delta + 14\sigma^3)}{30}\right)$ and γ is the magnetogyric ratio. β, the degree of stretching, is an empirical parameter that introduces the effects of polydispersity. $\beta = 1$ for monodisperse behaviour, but decreases with increasing polydispersity. It was necessary to incorporate a small degree of polydispersity to obtain the best fits, although this has little effect on the diffusion coefficients obtained.

Small-angle neutron scattering (SANS)

SANS experiments were performed on both the time-of-flight spectrometer LOQ on ISIS at the Rutherford Appleton Laboratories, Chilton, Didcot, Oxfordshire, and on D11 at the Institute Laue-Langevin, Grenoble, France.

Samples were contained in 5-mm path length UV-grade quartz cells. At ISIS the samples were kept at 20°C in the thermostatted sample changer, on D11 the experimental temperature was 23 ± 3°C. The raw scattering data were placed on an absolute scale according to the accepted procedures for each instrument. The scattering length densities (Higgins & Benoit 1994) of the various fluorinated solvents are typically 2–3 × 10^8 cm^{-2}, closely matched to that of PVP ($\rho_{sld} = 2.7 \times 10^8\,cm^{-2}$), hence the observed scattering arises predominantly from the PEG (ρ_{sld} $0.6 \times 10^8\,cm^{-2}$). Due to the small size of the polymers and the relatively weak contrast, samples took up to 2 h to obtain good statistics on LOQ, and a total of ~50 min on D11.

The data were fitted to a model for a polydisperse Gaussian coil, given by equation 2.

$$I(Q) = S_0 \frac{\left[1 + \frac{\left[(QR_g)^2\right]}{1+2(p-1)}\right]^{\frac{-1}{p-1}} + \frac{(QR_g)^2}{1+2(p-1)}}{p\left[\frac{\left[(QR_g)^2\right]}{1+2(p-1)}\right]^2} + B_{inc} \qquad (2)$$

where R_g is the radius of gyration and p is the sample polydispersity (1 = monodisperse). As with the PGSE-NMR it was necessary to incorporate a small degree of polydispersity (10–15%) to obtain good fits, although varying this number again had little effect on the final value of R_g. S_0 is a term that embodies the concentration of the sample, and the difference in the scattering length density of the polymer and solvent. B_{inc} is the incoherent background scattering.

Statistical methods

For the phase diagram experiments, a minimum of three measurements were taken at each temperature except where stated, and the quoted value is a simple average of these. However, the resolution in these experiments is different to the standard deviation of the average of the experimental points. For example, in the PEG temperature-phase behaviour studies, samples were examined in increments of 1 wt% polymer; the concentrations are known to a high precision, but the increment in the polymer concentration defines the overall resolution of the parameter obtained. Representative error bars are included in all raw data.

For the solubility measurements, duplicate samples were employed and results are an average of these. For the NMR experiments all data are shown. For the SANS experiments, duplicate measurements are not possible; the fitted value is derived from a non-linear least squares analysis of the data, with data point weighting corresponding to the relative magnitude of the error bar.

Results

Phase behaviour

A strong molecular weight dependence of PEG solubility is observed in these fluorinated solvents, with polymers above ~1000 g mol^{-1} being essentially insoluble (< 1 wt% solubility discernible by a dry weights analysis). At 20°C the solubilities were 40.0, 10.1, 0.05 and 0 wt% (±0.005 wt%) for PEG 600, PEG 1000 and for the PEG samples with 2000 g mol^{-1} and PEG 4600 g mol^{-1}, respectively. Hence this study was limited to two sizes of PEG, those samples denoted PEG 600 and PEG 1000, combined with PVP K25 and PVP K30.

PEG 600 in HPFP

At up to 30°C, PEG 600 was miscible with HPFP over the entire concentration region studied in detail, i.e. the solubility limit is unknown, but above 20 wt%. Above 30°C a monotonic decrease in the maximum polymer solubility with temperature was observed, solubility falling to 8 (±0.5) wt%, 5 (±0.5) wt% and 4 (±0.5) wt% at 35, 40 and 45°C, respectively. Above the phase boundary, cloudy solutions separated over time to give two clear layers. A dry weights analysis of the phase compositions at 40°C gave the following results: for a 15 (±0.05) wt% solution the upper phase constitutes 18 (±2) wt% of the sample volume, but contained 49 (±1) wt% polymer, whilst the lower phase concentration was 9 (±1) wt% polymer. For a 20 (±0.05) wt% solution, the polymer concentrations were 67 (±2) wt% and 6 (±1.5) wt% for the upper and lower phases, respectively, with the upper phase occupying 33 (±3) wt% of the volume. This indicates typical cloud-point-type behaviour at the phase boundary (Clint 1992). These results were identical, within experimental error, to those obtained in a repeat experiment using previously dried solvent.

PEG 1000 in HPFP

PEG 1000 showed a more complex temperature dependence of the phase behaviour, as illustrated in Figure 1. On heating, a large increase in the maximum solubility occurred between 28 and 32°C, and a sharp decrease between 35 and 40°C. Below 35°C biphasic samples consisted of a clear solution with floating solid polymer. Above 35°C, biphasic samples existed as two colourless

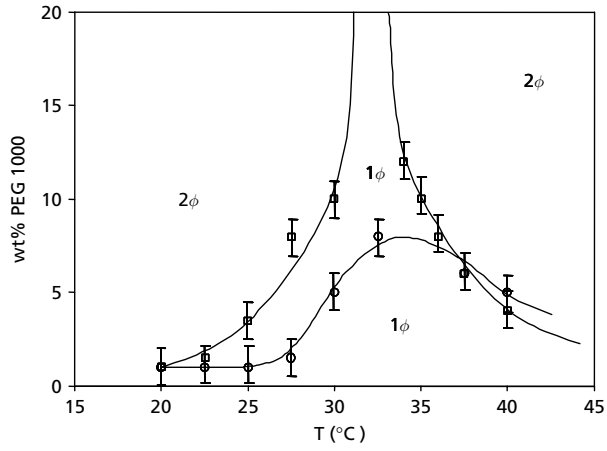

Figure 1 Phase diagram for PEG 1000 in HPFP. Heating curve (open circles), cooling curve (open squares). Lines are a guide to the eye.

liquid phases that turned cloudy on shaking. It is immediately obvious from Figure 1 that the phase behaviour on cooling is very different to that on heating. Once heated above 35°C a narrow temperature range (~32–35°C) exists where at least 20 wt% polymer may be solubilized (higher concentrations were not investigated). On reheating, the solubility limit reproduced the cooling curve. Clearly once the system is taken above 35°C there is an irreversible change in the phase behaviour, at least over the experimental timescales. The observed behaviour can be explained by the melting point of the polymer (36.5–38°C for this batch); once melted the polymer dissolves in the solvent and remains in solution on cooling. It is also possible that this is merely a kinetic effect, although best efforts indicate that these systems should be at equilibrium, and that PEG 1000 would eventually dissolve to the same degree regardless of its thermal history. However, solubilization behaviour this slow has important consequences for practical applications of these types of system, and therefore from a technical perspective the 'irreversibility' of the phase behaviour observed here is of immense practical relevance.

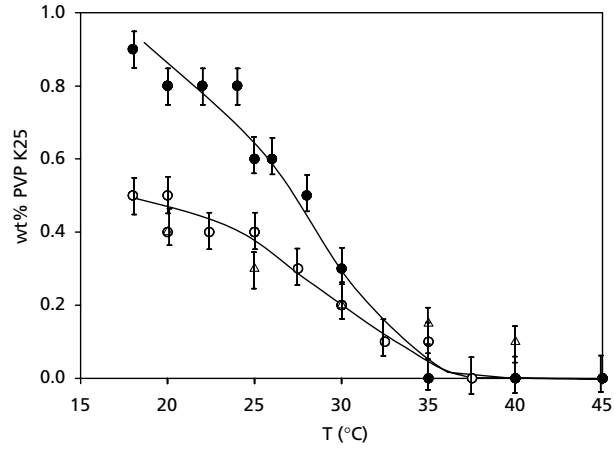

Figure 2 Phase diagram for PEG 600/PVP mixtures in HPFP at fixed PEG concentration. 3 wt% PEG 600/PVP K25 (open circles); 3 wt% PEG 600/PVP K30 (open triangles); 6 wt% PEG 600/PVP K25 (closed circles). Lines are a guide to the eye only.

PVP K25 and PVP K30 in HPFP

The solubilities of PVP K25 and K30 alone in HPFP are much lower. The lowest concentration sample analysed by visual inspection (0.5 wt%) remained as a two-phase system (clear solution with floating polymer) up to 40°C (the highest temperature investigated). Below this concentration the amount of polymer was difficult to detect visually and so a UV method was used to determine an accurate value of the solubility. At 25°C the solubilities of PVP K25 and PVP K30 in HPFP were 0.1 wt% (±0.02) and 0.01 (±0.006) wt%, respectively. By comparison, PEG 600 is miscible in all proportions with HPFP at 25°C. On addition of PEG to PVP/HPFP systems, a dramatic increase in PVP solubility is observed, as described below.

Mixed polymer systems

The phase behaviour of PVP/PEG solutions was studied at a fixed PEG 600 concentration of 3 wt%. This concentration was chosen such that PEG alone would remain in solution across the entire temperature range. The phase behaviour obtained is shown in Figure 2 and indicates a maximum solubility ratio at 15°C of 6:1 wt% PEG:PVP K30. The same result was obtained from experiments at 6 wt% PEG. The solubility of PVP is enhanced by the addition of PEG to the system. As shown in Figure 2, there was no significant change in the behaviour on switching from PVP K25 to PVP K30. This is perhaps unsurprising, considering the relatively small difference in molecular weight between the two different PVPs, compared to the large molecular weight difference between the PVPs and the PEGs.

PGSE-NMR

In order to investigate any interactions between the two types of polymer, PGSE-NMR was used to obtain the self-diffusion coefficient of PEG 600. PVP K25 was added incrementally to approach the phase boundary at a fixed temperature (25°C). The decay in the NMR signal intensity was followed for the PEG peak. This decay was fitted to a stretched exponential decay using the CORE analysis program (Stilbs et al 1996) to yield the self-diffusion coefficient (D_s) via equation 1. At 3 wt% PEG in HPFP a value of $D_s = 3.5 \times 10^{-12}\,m^2\,s^{-1}$ was obtained, which, compared with the aqueous case ($D_s = 3.0 \times 10^{-12}\,m^2\,s^{-1}$), is typical of a polymer of this size. No significant change in the measured diffusion coefficient was observed on adding PVP K25 at 0.01–0.5 wt% (i.e. up to the solubility limit). This indicates that there are no large changes in polymer conformation on addition of PVP and there is no evidence for physical association of the two polymers. This would have been manifested by a drop in self-diffusion coefficient of the PEG on addition of PVP as the much larger PVP would retard PEG mobility in solution.

Effect of water on phase behaviour

The influence of water on the phase behaviour of PEG in HPFP is best illustrated in Figure 3. Water was added incrementally to samples at a fixed concentration of PEG 600 in previously dried HPFP. The samples were examined by visual inspection after equilibration at a fixed temperature of 25°C. Above the phase boundary the samples form cloudy solutions from which water separates as droplets. These solutions became turbid again on shaking, indicating the formation of an emulsion. The experiment was repeated at various polymer concentrations and results show that water solubility scaled with polymer content (see inset). It is proposed that water could bind to the polymer, e.g. via hydrogen bonding, or simply that the water is more soluble in the polymer-rich solutions than in the pure solvent. From Figure 3 it

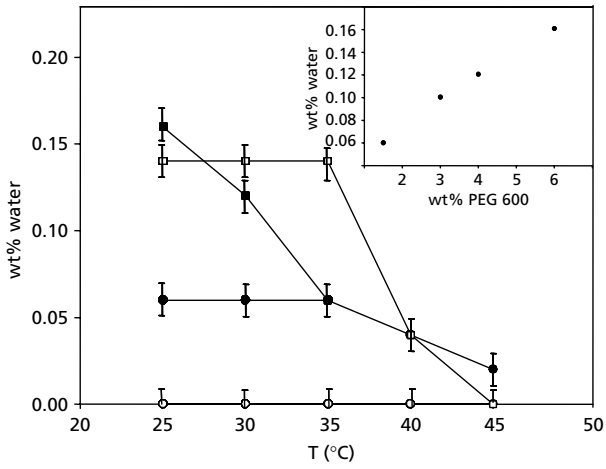

Figure 3 Phase diagram of PEG 600 solutions in HPFP with added water. PEG 600 concentrations were 0 wt% (open circles), 1.5 wt% (closed circles), 3 wt% (open squares) and 6 wt% (closed squares). Typical error bars are shown.

is possible to determine the maximum polymer:water ratio, which for PEG 600 is 35 (±5):1 by mass. At 6 wt%, the polymer itself starts to come out of solution without water being present, as seen in the earlier phase behaviour studies. In theory it would be possible to determine the location of the water by PGSE-NMR as the diffusion coefficient of free water (for example, if the water is dispersed in large droplets, as in an emulsion) would be much larger than that of water associated with the polymer. In practice, however, the water concentrations are too low to investigate.

The solubility of PVP increases from 500 ppm to 5000 ppm once the solvent is dried; however, for mixed polymer systems the water tolerance is still substantially lower than for PEG alone. Five microlitres of water was added to 3 mL of 2000 ppm solution of PEG 600 in dry HPFP to give a final concentration of 0.167 wt%, polymer:water ratio 1.2:1. This sample remained stable, whilst phase separation occurred on addition of 5 μL water to a comparable sample containing 2000 ppm PEG 600 and 2000 ppm PVP K25.

Mixed solvent systems

To investigate the influence of solvent polarity on polymer solubility, a series of experiments were performed with PEG 600. Its phase behaviour was studied at a fixed temperature (25°C) in HPFP/PFP and HPFP/PFD mixtures. In the absence of polymer the solvent pairs are miscible in all proportions. PEG 600 is insoluble in pure PFP and PFD but solubility is achieved by incorporation of large amounts of (dried) HPFP. At 25°C the solvent compositions (wt% HPFP) required to solubilize 5 wt% of PEG 600 were 90% with added PFP and 94% with added PFD (i.e. at greater than 10 wt% PFP and 6 wt% PFD 5 wt% PEG was not soluble).

Polymer conformation

PGSE-NMR was used to provide an estimate of the size of the polymer in solution via the self-diffusion coefficient. The hydrodynamic radii (R_h) were obtained from the diffusion coefficient via the Stokes–Einstein equation (equation 3) where k is the Boltzmann constant, T is the temperature, D_s is the diffusion coefficient and η is the solvent viscosity:

$$R_h = \frac{kT}{6\pi D_s \eta} \tag{3}$$

The expected concentration dependence of the measured D_s values was observed, D_s ranging from $4 \times 10^{-12}\,m^2\,s^{-1}$ at 2 wt% PEG 600 in HPFP to $0.7 \times 10^{-12}\,m^2\,s^{-1}$ at 22.5 wt% polymer. No change was observed on addition of PVP to the system.

SANS

SANS experiments were performed to obtain the radii of gyration of the PEG 600 in various solutions. Typical scattering data are shown in Figure 4.

To determine the radii of gyration (R_g) the raw data were fitted to a model for a polydisperse Gaussian coil, given by equation 2. Typical fits to the data are shown in Figure 4. The R_g values thus obtained for various PEG concentrations are plotted with R_h from the relevant PGSE-NMR data in Figure 5. As with the PGSE-NMR experiments, no significant change in behaviour was observed on addition of PVP to a solution of PEG 600. Adding PVP to a PEG solution in HPFP at fixed PEG concentration led to no change in R_g.

To investigate the effects of solvent quality two solvent blends were considered: HPFP/PFP and HPFP/PFD. Figure 6 shows the data and fits for HPFP/PFP mixtures. Inset are the radii of gyration obtained from the fits to equation 2, as a function of solvent composition for HPFP/PFP and HPFP/PFD mixtures.

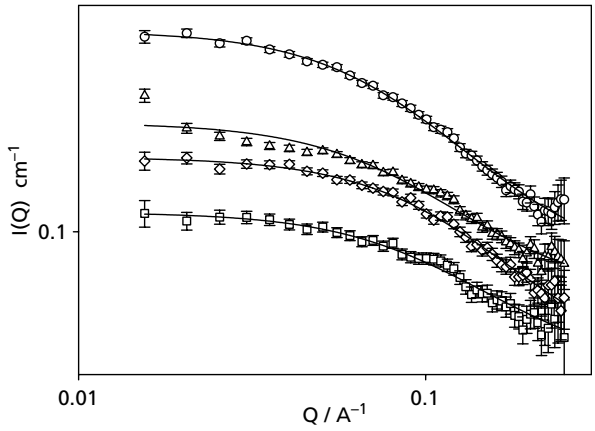

Figure 4 SANS data from PEG 600 solutions in HPFP. Concentrations were 9 wt% (open circles), 7.5 wt% (open triangles), 5 wt% (open diamonds), 4 wt% (open squares).

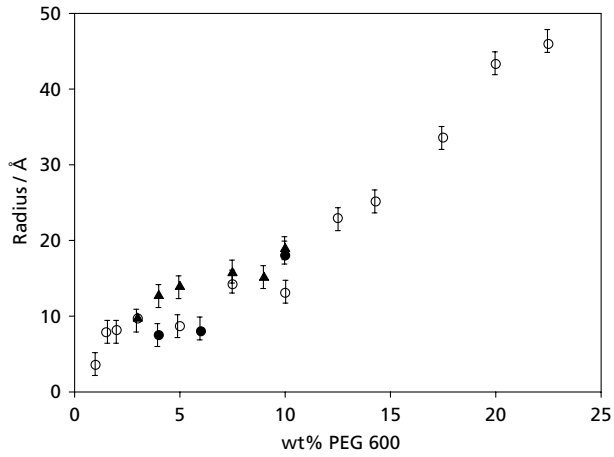

Figure 5 Hydrodynamic radii (R_h) obtained from PGSE-NMR for PEG 600 solutions in HPFP (open circles) and D_2O (closed circles). Also shown are radii of gyration (R_g) for PEG 600 in HPFP obtained from SANS experiments (closed triangles). Typical error bars are shown for each data set (±2 Å).

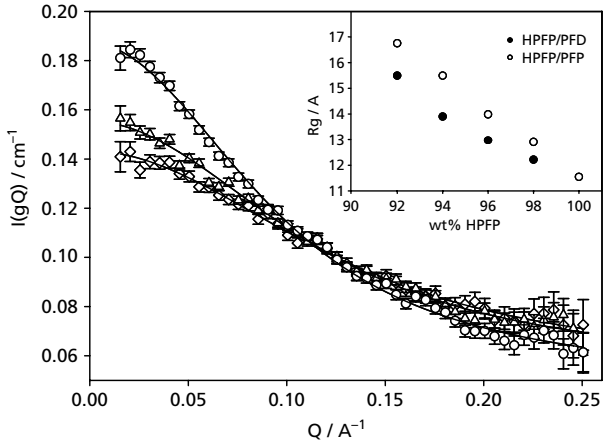

Figure 6 SANS data (symbols) and fits to Gaussian coils model (lines) for PEG 600 solutions in HPFP/PFP mixtures. 100/0 (diamonds), 98/2 (triangles), 94/6 (circles). Inset shows fitted R_g in HPFP/PFP (open circles) and HPFP/PFD (closed circles).

Molecular modelling was used to investigate the interaction between PEG and HPFP or PFP. Calculations were carried out at the B3LYP/6–31 + G** level in Gaussian03 (Frisch et al 2003). For the HPFP solvent case the system was set up with an oxygen–H(HPFP) interaction distance of 1.325 Å. After optimization this interaction distance extended to 2.178 Å, maintaining a weak hydrogen bonding interaction between solvent and monomer. The calculated interaction energy for this complex was $-16\,kJ\,mol^{-1}$, indicating a favourable interaction. For the PFP solvent case the optimized structure from HPFP/monomer dimer was altered by substitution of H with F. On optimization this complex completely dissociates to give a structure with the closest F–O interaction at 3.2 Å. This supports the phase behaviour studies in demonstrating that hydrogen bonding ability is the driving force behind polymer solubility.

Discussion

The type of phase separation at elevated temperatures observed for PEG is analogous to that found in aqueous solutions, i.e. a lower critical solution temperature is observed. This suggests that temperature-dependent intermolecular forces akin to hydrogen bonding govern polymer solubility.

The molecular weight dependence of PEG solubility has been observed previously in the partitioning of PEG between water and organic solvents. There is a transition in the observed behaviour as the molecular weight goes through a nominal value of about the same (Spitzer et al 2002) or slightly higher (Spitzer et al 2002) ($\sim$2000 g mol^{-1}). Spitzer et al (2002a, b) suggest that this may imply that solubility is dependent on the ability of the polymer to hydrogen bond with the solvent via the terminal hydroxyl groups, an effect that becomes diluted as polymer molecular weight increases. The strong molecular weight dependence in solubility observed in HPFP suggests hydrogen bonding to terminal OH groups on the polymer may be an important factor here. Additionally, for these fluorosolvent systems there may be a contribution from hydrogen bonding between H atoms in the solvent molecules (which are likely to be highly acidic due to the electron-withdrawing effects of the adjacent fluorine atoms) and lone pairs on the PEG oxygen atoms, and this is supported by the computer modelling data. Solubility studies in the mixed solvent systems indicate that hydrogen bonding interactions are the driving force behind polymer solubility in the fluorinated systems studied here. Unlike HPFP neither PFP nor PFD are capable of hydrogen bonding and a significant drop in polymer solubility is observed on replacing HPFP with either of the perfluorinated solvents.

At equivalent polymer concentration, the polymer radii observed by both PGSE-NMR and SANS in HPFP and water are similar so there is no evidence for aggregation of polymer chains. Interestingly, however, the SANS results show an *increase* in R_g as the amount of HPFP decreases for the mixed solvent systems. The same trend is observed whether we consider the solvent composition in terms of wt%, vol% or mol% HPFP. As the solvents added are fully fluorinated and unable to form hydrogen bonds with the polymer, it is expected that the affinity of the polymer for the solvent decreases and a lower R_g would be expected. It is possible that the enhanced scattering at low Q is due to an attractive interaction on approaching the phase boundary, rather than the influence of the solvent. This suggestion is supported when we consider the PGSE-NMR and SANS studies of PEG 600 at different concentrations in HPFP. The increase in observed radii with increasing polymer concentration (R_g or R_h) means that the polymer is less tightly coiled, i.e. there is a higher

compatibility with the solvent as more PEG is added. To cross check the SANS data in mixed solvent systems we carried out PGSE-NMR experiments on PEG 600 in 100% HPFP, 95% HPFP/PFP and 95% HPFP/PFD. The radii obtained in the mixed polymer systems were smaller than that in pure HPFP, consistent with a contraction of the polymer as the hydrogen bonding ability of the solvent decreases.

In mixed polymer systems it is clear that phase behaviour results are dominated by the larger, more solvophobic PVP. However, PEG clearly enhances PVP solubility in HPFP. In general, two synthetic polymers dissolved in a common solvent are expected to be mutually incompatible (Paricaud et al 2003), whereas in these systems a degree of synergy is observed, although there are other systems that do show such behaviour (Lewandowska 2005). PGSE-NMR experiments, however, showed no interaction between the polymers. This strongly suggests that PEG promotes PVP solubility by moderating the solvent properties.

The maximum amount of water solubilized in PEG/HPFP mixtures (an average of 35 wt%:1 wt% PEG:H_2O) equates to approximately 0.07 water molecules per ethylene oxide group, much lower than values reported in aqueous solution (typically one to six molecules of water per ethylene oxide group) but typical for various organic solvents (Tsai et al 1993; Spitzer et al 2002b).

Conclusions

The solubility of poly(ethylene glycol) in HPFP has been found to be strongly dependent on molecular weight, with polymers above *c*. 1000 g mol^{-1} showing very limited solubility. PEG exhibits a cloud-point-type temperature dependence of the phase behaviour. PGSE-NMR and SANS experiments showed a concentration dependence of the polymer size adopted in solution, indicating that the polymer moderates the solvent quality. This is supported by PGSE-NMR experiments using solvent mixtures comprising HPFP and the fully fluorinated liquids PFP and PFD. In mixed polymer systems PGSE-NMR experiments showed no evidence that any specific interaction was present between PEG and PVP, accordingly the increase in solubility of PVP in the presence of PEG is attributed to moderation of the solvent properties. The addition of even small amounts of water brings about phase separation. Clearly there is a need for closer study of the various solvent–solute interactions involved in order to fully understand behaviour in these systems.

References

Chaimberg, M., Cohen, Y. (1991) Free-radical graft polymerization of vinylpyrrolidone onto silica. *Ind. Eng. Chem. Res.* **30**: 2534

Clint, J. H. (1992) *Surfactant aggregation*. Blackie & Son, Glasgow

Frisch, M. J. Gaussian 03, Revision B.04, M. J. Frisch, G. W. Trucks, H. B. Schlegel, G. E. Scuseria, M. A. Robb, J. R. Cheeseman, J. A. Montgomery, Jr., T. Vreven, K. N. Kudin, J. C. Burant, J. M. Millam, S. S. Iyengar, J. Tomasi, V. Barone, B. Mennucci, M. Cossi, G. Scalmani, N. Rega, G. A. Petersson, H. Nakatsuji, M. Hada, M. Ehara, K. Toyota, R. Fukuda, J. Hasegawa, M. Ishida, T. Nakajima, Y. Honda, O. Kitao, H. Nakai, M. Klene, X. Li, J. E. Knox, H. P. Hratchian, J. B. Cross, C. Adamo, J. Jaramillo, R. Gomperts, R. E. Stratmann, O. Yazyev, A. J. Austin, R. Cammi, C. Pomelli, J. W. Ochterski, P. Y. Ayala, K. Morokuma, G. A. Voth, P. Salvador, J. J. Dannenberg, V. G. Zakrzewski, S. Dapprich, A. D. Daniels, M. C. Strain, O. Farkas, D. K. Malick, A. D. Rabuck, K. Raghavachari, J. B. Foresman, J. V. Ortiz, Q. Cui, A. G. Baboul, S. Clifford, J. Cioslowski, B. B. Stefanov, G. Liu, A. Liashenko, P. Piskorz, I. Komaromi, R. L. Martin, D. J. Fox, T. Keith, M. A. Al-Laham, C. Y. Peng, A. Nanayakkara, M. Challacombe, P. M. W. Gill, B. Johnson, W. Chen, M. W. Wong, C. Gonzalez, J. A. Pople, Gaussian, Inc., Pittsburgh PA, 2003

Griffiths, P. C., Stilbs, P., Paulsen, K., Howe, A. M., Pitt, A. R. (1997) FT-PGSE NMR study of mixed micellization of an anionic and a sugar-based nonionic surfactant. *J. Phys. Chem. B* **101(6)**: 915–918

Higgins, J. S., Benoit, H. C. (1994) *Polymers and neutron scattering*. Clarendon Press, Oxford

Krafft, M. P. (2001) Fluorocarbons and fluorinated amphiphiles in drug delivery and biomedical research. *Adv. Drug Deliv. Rev.* **47**: 209–228

Krafft, M. P., Riess, J. G. (1998) Highly fluorinated amphiphiles and colloidal systems, and their applications in the biomedical field. A contribution. *Biochemie* **80**: 489–514

Krafft, M. P., Reiss, J. G., Weers, J. G. (1998) The design and engineering of oxygen-delivering fluorocarbon emulsions In: Benita, S. (ed) *Submicronic emulsions in drug targetting and delivery*. Harwood Academic Publishers, Amsterdam, pp 235–333

Lide, D. R. (eds) (1994) *CRC handbook of chemistry & physics*, 75th edn, CRC Press, London

Lewandowska, K. (2005) The miscibility of poly(vinyl alcohol)/poly(N-vinylpyrrolidone) blends investigated in dilute solutions and solids. *Eur. Polymer. J.* **41**: 55–64

Paricaud, P., Galindo, A., Jackson, G. (2003) Understanding liquid–liquid immiscibility and LCST behaviour in polymer solutions with a Wertheim TPT1 description. *Mol. Phys.* **101**: 2575–2600

Reed, T. M. (1964) Physical chemistry of fluorocarbons. In: Simmons, J. H. (ed) *Fluorine chemistry*. Academic Press, New York, pp 133–221

Riess, J. G. (1994) Highly fluorinated systems for oxygen transport, diagnosis and drug delivery. *Colloids Surf.* **84**: 33–48

Riess, J. G. (2002) Fluorous micro- and nanophases with a biomedical perspective. *Tetrahedron* **58**: 4113–4131

Riess, J. P., Krafft, M. P. (1999) Fluorocarbons and fluorosurfactants for in vivo oxygen transport (blood substitutes), imaging, and drug delivery. *Mat. Res. Soc. Bull.* **24**: 42–48

Rigby, H. A., Bunn, C. W. (1949) A room-temperature transition in polytetrafluoroethylene. *Nature* **164**: 583–585

Rogueda, P. G. A. (2003) HPFP, a model propellant for pMDIs. *Drug Dev. Ind. Pharm.* **29**(1): 39–49

Spitzer, M., Sabadiini, S., Loh, W. (2002a) Poly(ethylene glycol) or poly(ethylene oxide)? Magnitude of end-group contribution to the partitioning of ethylene oxide oligomers and polymers between water and organic phases. *J. Braz. Chem. Soc.* **13**: 7–10

Spitzer, M., Sabadiini, S., Loh, W. (2002b) Entropically driven partitioning of ethylene oxide oligomers and polymers in aqueous/organic biphasic systems. *J. Phys. Chem. B.* **106**(48): 12448–12452

Stilbs, P., Paulsen, K., Griffiths, P. C. (1996) Global least-squares analysis of large, correlated spectral data sets: application to component-resolved FT-PGSE NMR spectroscopy. *J. Phys. Chem.* **100**(20): 8180–8189.

Tsai, R.-S., Fan, W., Tayar, N. E., Carrupt, P.-A., Testa, B., Keir, L. B. (1993) Solute–water interactions in the organic phase of a biphasic system. 1. Structural influence of organic solutes on the 'water-dragging' effect. *J. Am. Chem. Soc.* **115**: 9632–9639

Wolfson, M. R., Greenspan, J. S., Shaeffer, T. H. (1996) Pulmonary administration of vasoactive substances by perfluorochemical ventilation. *Paediatrics* **97**: 449–455